JJMIE

Volume 3, Number 4, December 2009
ISSN 1995-6665
Pages 272 - 279

Jordan Journal of Mechanical and Industrial Engineering

Vibration Analysis of Plates With Spot Welded Stiffeners

S. M. Nacy *, N. K. Alsahib, F. F. Mustafa

Al-Khawarizmi College of Engineering, University of Baghdad, Jaderyia, Baghdad, Iraq

Abstract

In this work both theoretical and experimental investigation was carried out to study the effect of residual stresses on the vibrational characteristics of plates with spot welded stiffeners at different boundary conditions. Expressions of the exact frequency equation were derived. Finite element modeling (FEM) was adopted to predict the tendon force produced due to spot welding and to find the natural frequencies at different modes. Different experimental models were tested to backup the results obtained theoretically. It was found that both theoretical and experimental results are in good agreement.

Keywords: Stiffened Plates; Spot Welding, Residual Stresses; Vibration Analysis; Finite Element Analysis.

Nomenclature

a, b	Plate side length (mm)
D	Flexural rigidity of an isotropic plate (N.mm)
Dx,Dy	Flexural rigidity of an orthotropic plate in x and y directions
Dxy	Torsional rigidity of an isotropic plate
Gxy	Shear modulus of orthotrpic material
h	Plate thickness (mm),
Nx	Edge forces per unit distance (N/mm)
T	Kinetic energy of the element (W)
t	Time (sec)
U	Strain energy stored in complete plate (W)
Ub	Strain energy stored due to bending (W)
Ut	Strain energy stored due to twisting (W)
Ur	Strain energy stored due to concentrated force (W)
w	Displacement components in z directions
x, y	Cartesian coordinates
C-F-S-C	Clamped-Free-Simply-Clamped
ρ	Mass density (Kg/mm^3)
ω	Angular frequency (rad/S)
ωf , ωs	Angular frequency without and with residual stresses non dimensional frequency.λ

1. Introduction

The wide use of stiffened structural elements in engineering began mainly with the application of steel plates for hulls of ships, steel bridges and aircraft structures. Structures consisting of thin stiffened plates have now also found wide applications in modern industry. The stiffening usually have a small part of the total weight of the structure, substantially influence their strength and performance under different load conditions. Recently, [1- 3] studied the free vibration analysis of stiffened plates and shells, it was found that the stiffeners shape and distribution have great effect on the natural frequencies and mode shapes of the plate.

On the other hand, resistance spot welding is a process used for joining faying surfaces. Major advantages of resistance spot welding are high speed and suitability for automation. Many researches have been published regarding joining strength and residual stresses of spot welds [4 - 6].

The main objectives of this investigation is to study the effect of spot distribution and residual stresses, induced from spot welding, on the vibrational characteristics of plates with spot welded stiffeners at different boundary conditions. Expressions of the exact frequency equation were derived. Finite element modeling was adopted to predict the tendon force produced due to spot welding, and to find the natural frequencies and mode shapes. Different experimental models were tested to backup the results obtained theoretically.

1.1. Frequency Equation

Due to the existence of stiffeners, the stiffened plate is treated as an orthotropic material. The fundamental equation for small deflection theory of bending of thin plates is used to give details of the theoretical analysis of residual stresses that result from welding and its effect on the natural frequencies and mode shapes. The governing differential equation of deflection for an orthotropic plate, subjected to a force (N_x per unit length) acting on the edges of the plate , can be written as,

$$D_x \frac{\partial^4 w}{\partial x^4} + 2H \frac{\partial^4 w}{\partial x^2 \partial y^2} + D_y \frac{\partial^4 w}{\partial y^4} = N_x \frac{\partial^2 w}{\partial x^2} \quad (1)$$

Where, $H = D_{xy} + 2\,G_{xy}$,

* Corresponding author. somernacy@gmail.com.

and D_x , D_y , D_{xy} , G_{xy} represent the flexural and torsional rigidities of an orthotropic plate, respectively.

The analysis of deformation and stress in an elastic body can be accomplished by employing the energy method. Conjunction of energy method with Rayleigh's principle is used to obtain an approximation to the modal frequencies of transverse vibration of thin plate subjected to longitudinal mid plane tension N_x per unit width as shown in figure 1. For a small rectangular element of plate, the strain energy stored is the sum of the work done by the bending moment δU_b , twisting moment δU_t , and the mid plane force δU_r . If the maximum kinetic energy of the element is δT , then the angular frequency ω of the plate may be deduced from the energy equation, where the integrations are taken over the whole plate.

$$\int dU_b + dU_t + dU_r = \int dT \tag{2}$$

Eq. (2) can be written as follows,

$$\int_{-a}^{a}\int_{-b}^{b}\frac{1}{2}\{D_x(\frac{\partial^2 w}{\partial x^2})^2 + 2D_{xy}(\frac{\partial^2 w}{\partial x^2}\frac{\partial^2 w}{\partial y^2}) + 4G_{xy}(\frac{\partial^2 w}{\partial x \partial y})^2 + D_y(\frac{\partial^2 w}{\partial y^2})^2\}dxdy +$$

$$\frac{1}{2}N_x\{\int_{-a}^{a}\int_{-b}^{b}(\frac{\partial w}{\partial x})^2 dxdy - \int_{-a}^{a} 2b(\frac{\partial w}{\partial x})dx\} = \frac{1}{2}\rho h\omega^2 \int_{-a}^{a}\int_{-b}^{b} w^2 dxdy \tag{3}$$

Free, transverse vibrations of the structural system under study are governed by the differential system,

$$D_x \frac{\partial^4 w(x,y,t)}{\partial x^4} + 2H \frac{\partial^4 w(x,y,t)}{\partial x^2 \partial y^2} + Dy \frac{\partial^4 w(x,y,t)}{\partial y^4} + \rho h \frac{\partial^2 w(x,y,t)}{\partial t^2} = 0 \tag{4}$$

The displacement function w(x, y, t) is approximated by means of the expansion,

$$w(x,y,t) \approx w(x,y)\sin\omega t = \sin\omega t \sum_{ij} C_{ij} X_i(x) Y_i(y) \tag{5}$$

Table 1 shows expressions of the displacement function for different boundary conditions. Substituting each expression separately in eq.(3), integrating over the given domains, applying boundary conditions and rearranging terms to obtain the final form of the frequency equation as listed below,

$$a^4 \frac{\rho h}{D_x}\omega_f^2 = [C_1 + C_2 \frac{a^2}{b^2}(\frac{D_{xy} + 2G_{xy}}{D_x}) + C_3 \frac{a^4}{b^4}\frac{D_y}{D_x}] \tag{6}$$

and

$$\omega_s^2 = \omega_f^2 + A\frac{N_x}{\rho h a^2} \tag{7}$$

where C_1 , C_2 , C_3 and A are constants depending on the boundary conditions as tabulated in table 2. Sample of calculation of these constants is clarified in Appendix.

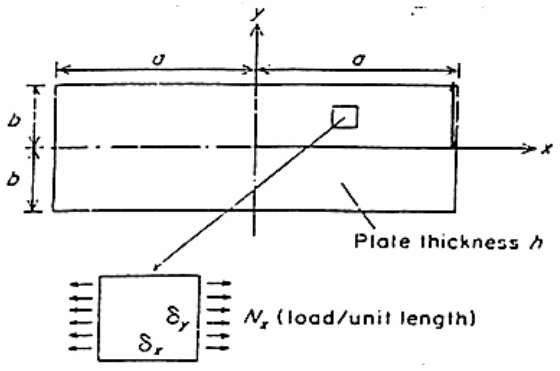

Figure 1. Geometry and mid-plan loading of a rectangular plate.

2. Finite Element Modeling

The FEM analysis was carried out in two steps (coupled-field analysis). A non-linear transient thermal analysis was conducted first to obtain the global temperature history generated during the welding process. A stress analysis was then developed with the nodal temperatures obtained from the thermal analysis, which are applied as "body force" in the subsequent stress analysis. Then by using the result from the stress analysis with pre-stress on, dynamic structural analysis was achieved. ANSYS software was implemented to achieve such a task. The accuracy of the FEM depends on the density of the mesh used in the analysis. Therefore, it was necessary to have a more refined mesh closer to the weld nugget, while in regions located away from weld-nugget a more coarse mesh was used, as shown in figure 2. After solving the non-linear transient heat transfer and residual stress model, modal analyses were achieved to determine the natural frequencies and mode shapes of a structure.

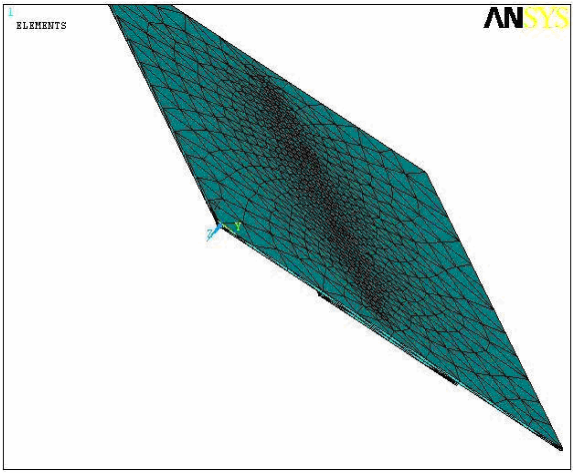

Figure 2. Finite element mesh.

3. Experimentation

Experimental tests were designed in order to measure the natural frequency and mode shape of the plates with spot welded stiffeners. A photograph of the instruments used is shown in figure 3, a simplified block diagram for the these instruments is presented in figure 4. The sheet

Table 1 Displacement functions.

Boundary Condition	Displacement Function
C-C-C-C	$w = C[(\frac{2x}{a})^2 - 1]^2[(\frac{2y}{b})^2 - 1]^2 \sin \omega t$
C-C-C-S	$w = C[(\frac{2x}{a})^2 - 1]^2[1 + \frac{y}{b} - 6(\frac{y}{b})^2 - 4(\frac{y}{b})^3 + 8(\frac{y}{b})^4] \sin \omega t$
C-S-C-S	$w = C[(\frac{2x}{a})^2 - 1]^2[1 - \frac{6}{5}(\frac{2y}{b})^2 + \frac{1}{5}(\frac{2y}{b})^4] \sin \omega t$
S-S-S-S	$w = C[1 - \frac{6}{5}(\frac{2x}{a})^2 + \frac{1}{5}(\frac{2x}{a})^4][1 - \frac{6}{5}(\frac{2y}{b})^2 + \frac{1}{5}(\frac{2y}{b})^4] \sin \omega t$
S-S-S-C	$w = C[1 - \frac{6}{5}(\frac{2x}{a})^2 + \frac{1}{5}(\frac{2x}{a})^4][1 + \frac{y}{b} - 6(\frac{y}{b})^2 - 4(\frac{y}{b})^3 + 8(\frac{y}{b})^4] \sin \omega t$
C-C-S-S	$w = C[1 + \frac{x}{a} - 6(\frac{x}{a})^2 - 4(\frac{x}{a})^3 + 8(\frac{x}{a})^4][1 + \frac{y}{b} - 6(\frac{y}{b})^2 - 4(\frac{y}{b})^3 + 8(\frac{y}{b})^4] \sin \omega t$
C-C-C-F	$w = C[(\frac{2x}{a})^2 - 1]^2[\frac{56}{17}(\frac{y}{b}) + \frac{24}{17}(\frac{y}{b})^2 - \frac{32}{17}(\frac{y}{b})^3 + \frac{16}{17}(\frac{y}{b})^4] \sin \omega t$
C-C-S-F	$w = C[1 + \frac{x}{a} - 6(\frac{x}{a})^2 - 4(\frac{x}{a})^3 + 8(\frac{x}{a})^4][\frac{56}{17}(\frac{y}{b}) + \frac{24}{17}(\frac{y}{b})^2 - \frac{32}{17}(\frac{y}{b})^3 + \frac{16}{17}(\frac{y}{b})^4] \sin \omega t$
S-C-S-F	$w = C[1 - \frac{6}{5}(\frac{2x}{a})^2 + \frac{1}{5}(\frac{2x}{a})^4][\frac{56}{17}(\frac{y}{b}) + \frac{24}{17}(\frac{y}{b})^2 - \frac{32}{17}(\frac{y}{b})^3 + \frac{16}{17}(\frac{y}{b})^4] \sin \omega t$

Table 2. Values of the constants C_1 , C_2 , C_3 , A

Boundary Condition	C_1	C_2	C_3	A
C-C-C-C	504	288	504	-17.531
C-C-C-S	504	272.83	238.73	-12.86
C-S-C-S	504	236.89	97.54	-11.44
S-S-S-S	97.54	194.87	97.54	-9.72
S-S-S-C	97.54	224.43	238.73	-10.586
C-C-S-S	238.73	258.48	238.73	-11.368
C-C-C-F	504	69.312	32.358	12
C-C-S-F	238.73	64.77	32.358	11.368
S-C-S-F	97.54	56.24	32.358	9.87

material employed in this investigation for all tests was an austenitic stainless steel AISI 304 sheet with nominal thickness of 0.6mm.

The welding process was implemented using the spot welding machine type (P1–Rectifier Press Spot Welding Machine Schlatter), with a force transducer, a displacement transducer, a Rogowski coil for measuring the welding current and a temporizer for controlling the welding cycle (squeezing, welding and holding times). The welding machine has a maximum force of 1,885 daN, a supply pressure of 6 bar and a nominal welding power of 200 KVA. The electrodes have a truncated conical shape with a flat circular contacting area of 5 mm diameter, made of pure copper, which has high

  - Volume 3, Number 4 (ISSN 1995-6665)

Figure 3. Measuring Instruments.

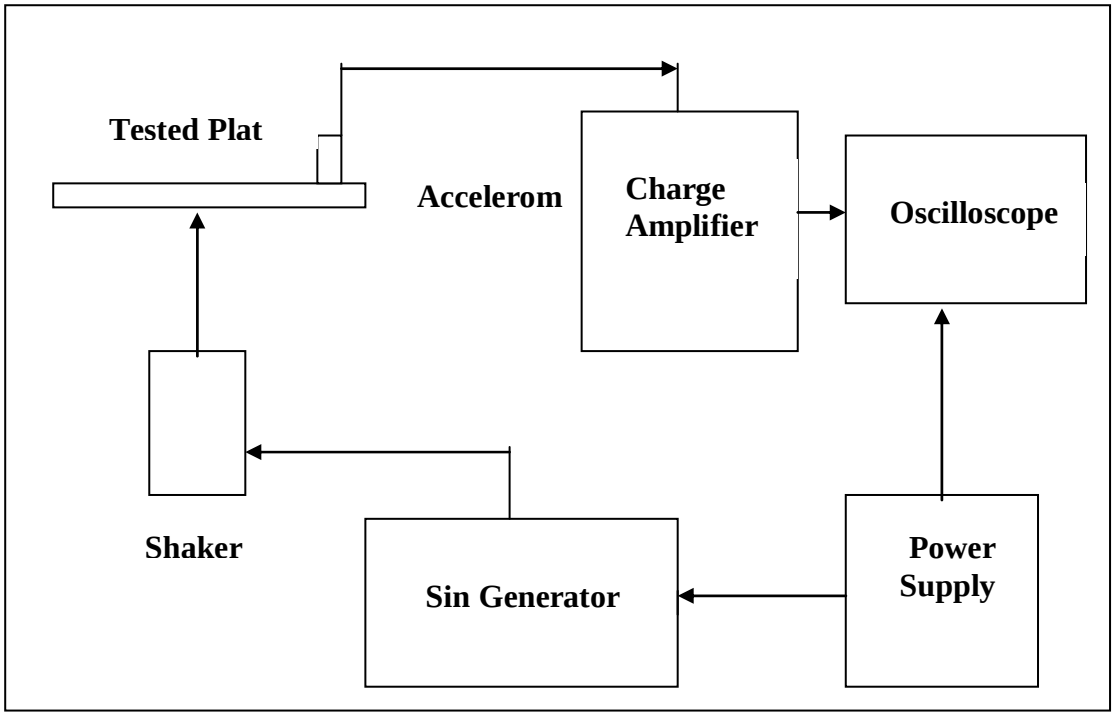

Figure 4. Block Diagram of the Measuring Instruments.

thermal and electrical conductivity, and were chosen in accordance with the ISO 5182 standard.

A rectangular stainless steel plate with dimensions of (120mm, 100mm, 0.6 mm) stiffened by another stainless steel plate of (120mm, 40mm, 0.6mm) in the longitudinal direction, is considered in this study. Five groups of plates prepared as the stiffened plate specimens, with different spot welding position are illustrated in figure 5.

The measurement of natural frequencies has been done with and without including the effect of residual stresses for each specimen to find the shift in this frequency due to spot welding.

The frequency response for each stiffened plate was investigated by slowly increasing the driving frequency of the vibrator by means of the sine generator. The natural frequency was distinguished by observing the

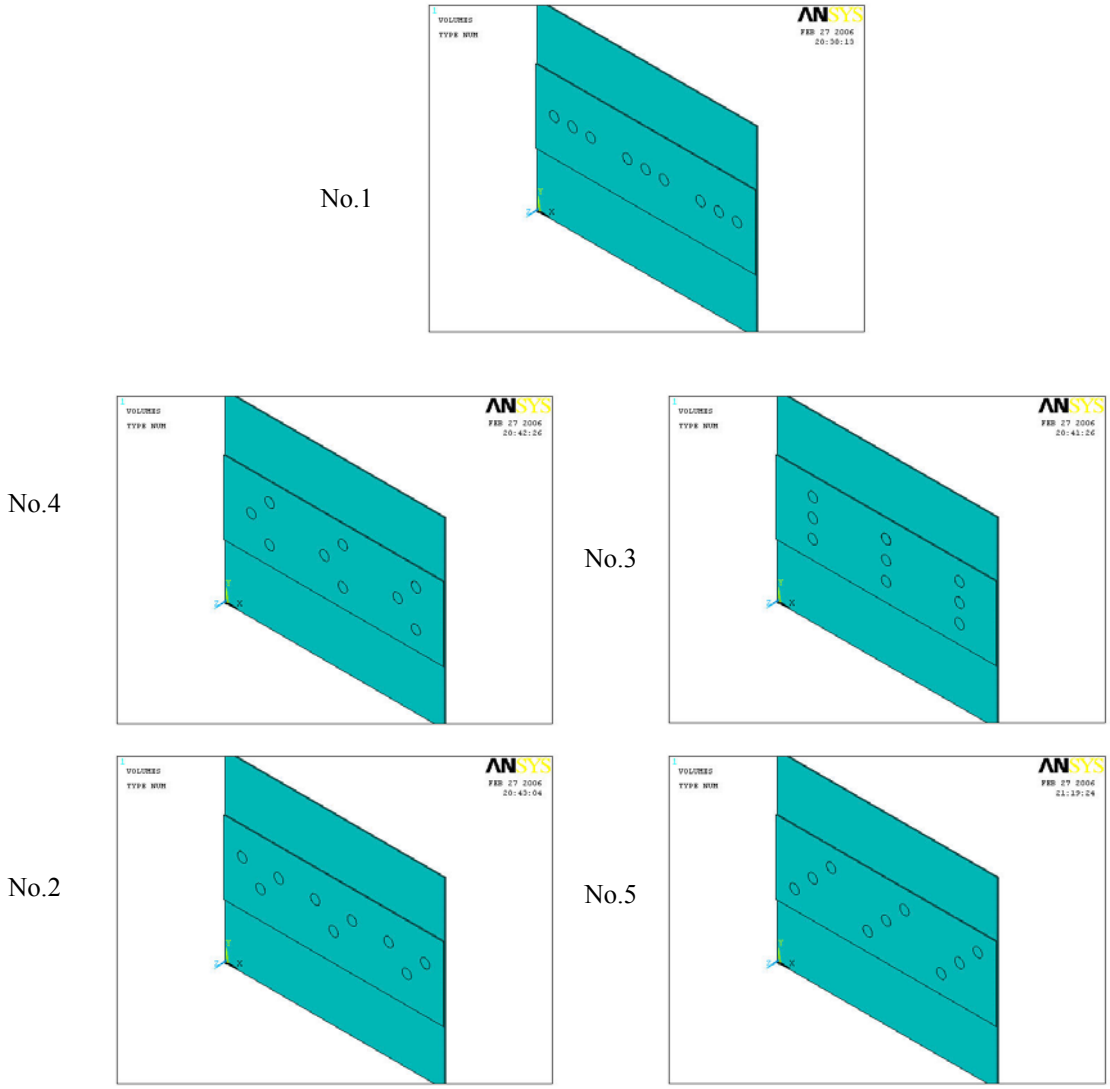

Figure 5. Different stiffened plate models.

sharp increase in amplified of the pickup output, which was amplified and displayed on the oscilloscope.

Heat treatment was employed to spot weld joint to investigate their effect on the natural frequency and mode shape of stiffened plate.

The stress reliving heat treatment was employed at a temperature of (750 C), for 3 minutes duration, then the weldments was cooled by air.

4. Results and Discussions

In order to clarify the results obtained from this investigation, three main effects were taken into consideration, namely, spot welds distribution, residual stresses and boundary conditions. Results are presented in tables 3 and 4. The first two natural frequencies for the five models considered in this study with a clamped-free-free-free boundary condition are tabulated in table 3. Although differences are small, but it is clear that the highest natural frequency is gained by model 5. Both numerical and experimental results insure that the inclusion of residual stresses tends to raise the natural frequency, for these stresses are mainly tensile in nature,

Table 3. Natural frequencies (Hz) for C-F-F-F boundary condition.

Model No.	Mode No.	FEA Results		Experimental Results	
		With Residual	Without Residual	With Residual	Without Residual
1	1st	73.934	69.949	69.2	65.5
	2nd	152.06	145.62	144.2	137.8
2	1st	72.895	68.84	67.9	63.8
	2nd	165.07	157.98	154.1	144.8
3	1st	74.329	70.363	69.8	65.6
	2nd	164.44	156.03	153	146.1
4	1st	73.241	69.166	70.1	67.2
	2nd	157.26	147.08	145.8	139
5	1st	74.3	71.046	69.5	65.7
	2nd	165.87	157.06	157.8	147.8

thus increasing the lateral stiffness of the plates, leading to an increase in natural frequency. The amount

of increase in natural frequency due to residual stresses is small because these stresses are acting on small areas (spots) as compared to the area of the plate.

Nodal line and mode shapes for model 1 with clamped-free-free-free boundary conditions are shown in figure 6. Mode shapes obtained numerically and experimentally are almost identical. The maximum difference in natural frequency happened to be in the first mode with a value of 6.841%, which is almost acceptable.

In order to verify the derived expressions for natural frequencies with and without the inclusion of residual stresses, values of the fundamental natural frequency for model 1 at different boundary conditions were calculated and listed in table 4. Natural frequencies obtained analytically and numerically are in good agreement, the maximum difference happened to be in the range of 1.7%. This indicates good proof for the validity of the derived frequency expressions.

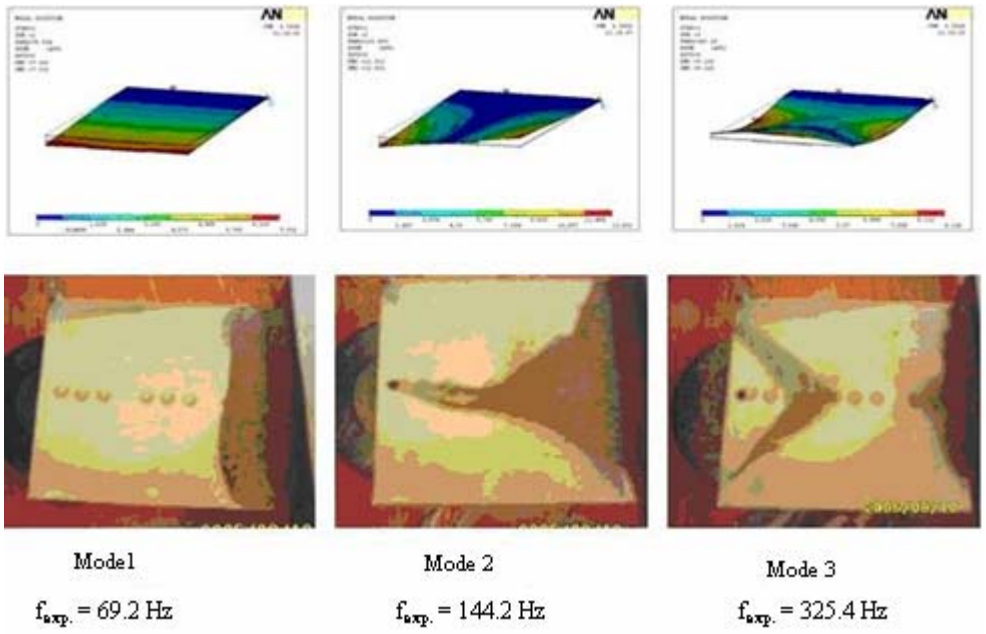

Figure 6. Nodal line and mode shapes of model 1 with C-F-F-F boundary condition.

Table 4. Fundamental natural frequencies (Hz) for different boundary conditions.

No.	B-C Description	Analytical Results			FEA Results		
		With Residual	Without Residual		With Residual	Without Residual	
1	C - C - C - C	775.153	773.963		770.797	768.3	
2	C-S-C-C	582.432	581.269		582.61	577.67	
3	C-S-C-S	443.812	442.454		437.91	436.39	
4	S-S-S-S	362.257	360.84		358.46	357.39	
5	S-C-S-S	522.304	521.23		520.63	518.65	
6	C-S-S-C	545.639	544.54		542.79	539.21	
7	C-F-C-C	372.397	370.698		366.06	363.06	
8	C-F-S-C	310.972	309.043		307.06	304.65	
9	S-F-S-C	267.60	265.659		264.35	263.12	

5. Conclusions

According to the results obtained, it can be seen that both theoretical and experimental results showed good agreement. It was found that residual stresses produced in each nugget have significant effect on the natural frequency of the plate, where natural frequency increases when residual stresses are included. This effect varies depending on the boundary conditions of the plate and on the distribution of the weld spots.

Refernces

[1] M. Guo, I.E. Harik, W.X. Ren, "Free vibration analysis of stiffened laminated plates using layered finite element method". Structural Engineering and Mechanics, Vol. 14, 2002, 245-262.

[2] Jung JY, Kim JH. Vibration control of stiffened plates with integrated piezoelectrics. School of Mechanical and Aerospace Engineering. Coll. of Engineering, Seoul, Korea; 2002.

[3] S.M. Nacy, M.Q. Abdullah, M.M. Ali, "Free vibration analysis of stiffened conical shell". Journal of Engineering, Coll. of Engineering, Vol. 8, 2002, 263-275.

[4] Berglund D, Runnemalm H. Comparison of deformation pattern and residual stresses in finite element models of a TIG-Welded stainless steel plate. Volvo Aero Corporation, Manufacturing Process Development, Sweden; 2002.

[5] D.H. Bae, I.S. Sohn, J.K. Hong, "Assessing the effects of residual stresses on the fatigue strength of spot welds". Welding Journal, 2003, 18-23.

[6] Xin L. Finite element analysis of residual stress generation during spot welding and its affect on fatigue behavior of welded j. Ph.D. Thesis, University of Missouri-Columbia, December; 2005.

Appendix

This appendix shows a sample of calculation for C_1,C_2 ,C_3 , and A for the case of C-C-C-C. Consider an approximate solution with one term

$$w = C[(\frac{2x}{a})^2 - 1]^2[(\frac{2y}{b})^2 - 1]^2 \sin \omega t$$

Satisfying the boundary conditions:

$$w = w_{x=\pm(a/2)} = 0$$

$$w = w_{y=\pm(b/2)} = 0$$

$$\frac{\partial w}{\partial x} = \frac{\partial w}{\partial x}_{x=\pm(a/2)} = 0$$

$$\frac{\partial w}{\partial y} = \frac{\partial w}{\partial y}_{y=\pm(b/2)} = 0$$

Substitution w(x,y))in eq (3) one obtains the following frequency equation.

$$a^4 \frac{\rho h}{D_x} \omega_s^2 = [504 + 288 \frac{a^2}{b^2}(\frac{D_{xy} + 2G_{xy}}{D_x}) + 504 \frac{a^4}{b^4} \frac{D_y}{D_x}] +$$

$$17.531 a^2 \frac{N_x}{D_x} = \lambda^2$$